NAU Journal of Civil Engineering (NAUJCVE) May/June 2024

Nnamdi Azikiwe University Journal of Civil Engineering (NAUJCVE)

Volume-2, Issue-2, pp-17-23
www.naujcve.com
Research Paper Open Access

Predicting First Crack Load on Hollow Cored Rectangular RC Beams Using Finite Element Method: A Validation

[1]Ogbonna Uche K., [2]Okonkwo Henry N.

[1]Department of Civil Engineering, University of Benin, Benin City, Edo State, Nigeria

[2]Department of Industrial safety and Environmental Technology, Petroleum Training Institute, Effurun, Warri, Delta State, Nigeria.

Corresponding Author : kingsley.ogbonna@uniben.edu

ABSTRACT:
To predict the first crack load of a hollow cored reinforced concrete (RC) beam element, a finite element equation validated by an experiment is developed. Experimentally, flexural testing with point loads at mid-span was performed on fifteen (15) beams made up of three (3) beam types at 1 kN intervals for a span of 750mm using the Universal Testing machine. The beams were simply supported by roller points. The dimensions of the beams were kept constant and later varied while investigating the following hollow diameters: 0, 30, 60, 75, and 105mm. Numerically, the beams were designed as a beam element point loaded at mid-span with a span of 700mm centers, and the support conditions were defined as pinned support. The numerical and experimental results were in good agreement and is well presented. The finite element equation was further validated by comparing the first crack load values obtained from literature. It was observed that the first crack load equation's results agreed well with that of the previous study carried out on hollow RC beam sections. On average, the value of the ratio of the analytical and finite element first crack load was 0.965, with a coefficient of variation of 2.58% and a standard deviation of 0.025. The finite element equation accurately predicts the RC hollow cored rectangular beams' first crack load..

Keyword: *Finite element method, First crack load, Hollow-cored Beam, Modulus of rupture, Moment of inertia*

I. INTRODUCTION

In other to reduce weight and provide electrical and mechanical services, hollow cored RC rectangular beams are used in roof beams. The opening in simply supported RC beams has been extensively studied through numerical modeling, experiments, and analytical derivation (Jithinbose et al; Osman et al, 2016). Ling et al., 2019 conducted an experimental study on reinforced concrete beams with circular transverse openings. The beams were evaluated in terms of the load-displacement responses, mechanical properties, deflections, and failure modes. About 20% of the beam strength was impacted by an opening whose diameter did not exceed 0.25 times the height of the beam without reinforcements at the entrance. For opening sizes no larger than one-third of the beam height, the diagonal bar strengthening method successfully restored the beam strength. The proposed equation model provided an estimate of the beam's ultimate capacity when it had a transverse opening.

Mohammed and Najim , 2020 investigated the viability of employing recycled concrete aggregates (RCA) to create self-compacting concrete (RASCC). The fractal theory was applied to image processing techniques in order to determine the pattern and propagation of the fractures. The fracture energy characteristics of surface fractures were also established. It was discovered that the tested beams with RCA incorporation showed a decline in strength, stiffness, and toughness that was consistent with the traditional definition of fracture energy.

An experimental investigation was conducted by Ling et al., 2020 to examine the behavior of RC beams having circular holes. They looked into how the beam performed in relation to the size, location, and type of opening, as well as the best way to reinforce it. The four-point load test was used to evaluate eleven RC beams. This comprised three beams with reinforced openings, six beams with openings, and two control beams without openings. The dimensions of the beam were 150 mm for width, 300 mm for height, and 1650 mm for length. There was a 1500 mm clear span between the supports. The first shear crack delayed and the shear crack that eventually reached the opening delayed as the opening size decreased from 100 mm to 50 mm. Under the flexural load, no delay was observed.Varying techniques of calculation can result in considerable differences in the computed ductility, especially when it comes to the first crack and load factor. This might lead to varying needs for the required ductility in order to ensure structural safety. Furthermore, not every method has clear needs, thus it's important to avoid applying requirements from one method to another arbitrarily.

A structure's ductility is essential to its safety since inadequate ductility can result in an abrupt, brittle failure. Despite its importance, there is no clear way to figure it out, which causes inconsistent results and uncertainty when choosing the right methods. Erroneously assessing a structure's malleable characteristics may lead to disastrous outcomes. Consequently, a number of pilot studies were reviewed in their study, and twenty-one different approaches to ductility index computation were found. These indices were divided into three categories: energy-based, displacement-based, and conventional. Conventional ductility indices are typically used for steel-reinforced members, energy-based ductility indices for static-load and earthquake-resistant buildings, and deformation-based ductility indices for FRP-reinforced components. The study's main objectives are to give readers an overview of the variety of ductility techniques that are available and to help them choose the best techniques for certain elements and structures. (Ling et al., 2023).

A mixed-mode I/II fracture criterion was introduced by Fakoor and Farid (2018) to examine the beginning of cracks in orthotropic materials when the cracks are directed along fibers. The fractured orthotropic materials were examined using an expanded version of the minimum strain energy density criterion. It is suggested that the reinforced isotropic solid model, which is based on collinear crack propagation along fibers, is a useful model for analyzing composite fracture behavior.In their model, fibers were introduced as reinforcements of the isotropic matrix in orthotropic materials. The impacts of these reinforcements were qualified at the tension and shear modes by the definition of reinforcement factors. The crack initiation phenomenon can be predicted by the suggested criterion. Consequently, a novel definition of linear fracture toughness for orthotropic materials was put forth in their work. The proposed criteria's result was validated through the use of experimental data. The effectiveness of the new criterion to forecast crack initiation in orthotropic materials was demonstrated by the coincidence of fracture limit curves and experimental data.

Zhang and Li (2004) used a superposition method to determine the fracture tip stress intensity factor. The basic material parameters for model input were the fracture toughness of hardened cement paste (K_{IC}) and the crack bridging law, often known as the stress-crack width (r-d) relationship of the material. Deformation-controlled three point bending tests were performed on two varieties of steel fiber concrete beams, namely straight (SSFRC) and hooked(HSFRC),in order to validate the aforementioned model.The SSFRC and HSFRC were round in shape, with diameters of 0.4 and 0.5 mm and lengths of 25 and 30 mm, respectively. The bending span was 400 mm, and the beam size was 420x100x100 mm. Elastic stage with a constant stiffness up to the first crack stress (r_{fc}), which is a function of K_{IC} and a_0. Phase one of the crack development process involved increasing the load and gradually reducing the beam stiffness until the crack length approaches 40% of the beam depth.

Agag et al., 2022 conducted an experiment to study the behavior of reinforced concrete beams with variously positioned openings as well as the effectiveness of various strengthening methods for these beams. Various strengthening techniques were applied, including the use of externally bonded CFRP sheets, additional diagonal steel bars, and upper and lower steel bars. Thirteen reinforced concrete beams with a cross section of 160 mm by 400 mm and a total length of 2400 mm, including 2200 mm of effective length, were cast. Up to a load of 101.5 kN, the load-mid span deflection data for the solid (control) beam, BN, demonstrated a linear behavior.

The first crack initiated at the load of 101 kN. This load was therefore regarded as the yielding load.The load-deflection curve failed to behave linearly after yielding until it reached a maximum point loading of approximately 142.5 kN.

Berrocal et al., 2020 investigated the application of distributed optical fiber sensors (DOFS) for structural health monitoring in civil engineering constructions. DOFS is based on optical frequency domain reflectometry of Rayleigh backscattering. More precisely, the findings were presented from a set of laboratory tests intended to evaluate the applicability and precision of DOFS for crack monitoring in reinforced concrete components exposed to external loading. The testing involved three-point bending tests on concrete beams, with an optical fiber sensor coated in polyamide directly glued to the surface of an unaltered reinforcement bar and shielded by a silicone layer. The DOFS system's strain readings showed a level of accuracy comparable to that of conventional electrical foil gauges.

Lia et al., 2020 proposed a method based on the Bažant Crack Band Model (CBM) and digital image correlation (DIC) technique to determine the crack tip position and fracture process zone (FPZ) in concrete. The method was as follows: the critical crack opening displacement of concrete (w_{cr}) was determined based on CBM and the fundamental mechanical properties; (2) the DIC method was used to obtain the displacement field on the specimens' surface; and (3) the crack tip position was defined as the position where the crack opening displacement equaled to w_{cr}. When the fatigue loading initiated in the fatigue crack propagation testing, the entire fatigue crack was FPZ until the non-cohesive crack developed and the length of FPZ decreased. When the number of loading cycles was approximately fifty percent of the fatigue life, the length of FPZ tended to stay steady.

Predictive numerical models for sandwich panel design must undergo extensive validation before being used with high confidence and dependability. Local displacement measurements have been used to confirm numerical bending models found in the literature; nevertheless, a complete validation of surface strain is absent. In order to thoroughly validate that numerical model, Vervloet et al. 2019 conducted four-point bending tests that were observed by a digital image correlation system and compared with it. Utilizing a digital image correlation (DIC) system for monitoring provided an extremely detailed picture of the behavior of the sandwich panel's various materials under strain and during bending. The measured strains confirmed the theoretical model predictions for the shear deformation of the core and multiple breaking of the TRC tensile face, among other things.

II. MATERIALS AND METHODS

A. Formulation of the First crack load equation

Numerically, the predicted failure load was obtained from the Numerical Relationship between the modulus of rupture and the Predicted Failure load P_f. Bharikatti (2005) presented a problem with a rectangular Beam element that is simply supported at both ends under axial point load using moment-curvature equations.

The formulation of the finite element equation is well presented in Orie and Ogbonna, 2024.

$$\{P_f\} = \frac{3.5}{yl_e}\{f_r\}\left[\frac{bh^3}{12} - \frac{\Pi R^4}{3.9275}\right] \quad (2.1)$$

Where $\{P_f\}$ = Numerical predicted failure load in KN
$\{f_r\}$ = Modulus of rupture in N/mm^2
I = Moment of inertia in mm^4
Y = depth of neutral axis from the topmost fiber in the tension zone in mm
$D_{min.}$= Minimum diameter of the hole for any known first crack load in mm
b = width of the beam in mm
h = depth of the beam in mm
l_e= *midspan length in mm*
$\{f_r\} = 0.7\sqrt{f_{ck}}$ (Portland Cement Association, 15th edition)

1. Concrete mix

Flexural testing was performed on the beams in the Laboratory with point loads at mid-span. The load from the universal testing machine was steadily increased until the first crack was observed. Readings were taken at 1kN intervals throughout the beam length. The beam length was taken to be 750mm. The hollow cored beams were made using a prescribed concrete mix proportion of 1:2:4 by weight with a water cement ratio of 0.5 at twenty eight (28) days. A characteristic strength, f_{cu} of 20N/mm^2 was produced from the mix proportion.

Tests were conducted on the cubes at 7, 14, and 28 days with the largest size of the crushed granite been 19 mm. The grade and properties of the coarse aggregate followed the guide lines provided in the COREN Publication on Concrete Mix Design (The Coren/2017/016/RC,2017). Zone 3 was used to grade the fine aggregate.The Dangote Cement Company's Portland limestone cement (P.L.C.) was used and classified as CEMII in accordance with NIS444-1, 2014. The minimal amount of reinforcement determined for the tensile zone was mild steel (2R6) top and bottom reinforcement. There were two leg, 6 mm diameter links at 200 spacing, The experimental setup is well presented in Orie and Ogbonna, 2024.

2. Beam Elastic modulus

The modulus of elasticity was calculated from BS 8110;

$$E_{c,28} = K_o + (0.2f_{cu,28}) \quad 2.2)$$

Where; $E_{c,28}$: the modulus of elasticity at 28 days;
$f_{cu,28}$: the characteristic cube strength at 28 days (in N/mm^2);
K : a constant closely related to the modulusof elasticity of the aggregate (taken as 20 kN/mm^2 for normal-weight concrete).

3. Beam Reinforcement

Mild steel (2R6) was provided in the tensile zone, being the minimum reinforcement deduced from Mosley and Bungey, 1990.

A. Numerical Validation

Consider A previous research carried out by Murugesan and Narayanan, 2016 where Thirteen (13) RC rectangular beam specimens were examined under two point loading. The first specimen was solid, and the remaining twelve had longitudinal circular holes of varying widths. The dimensions of the holes were 25, 40, and 50 mm. There was variation in the distance between the top face and the center of the hole, below, within, or outside the stress block. The thirteen rectangular beams were measured 1700mm x 150mm x 250mm. The distance of centre of hole from top surface in mm varied from 45 to 180mm.

The cracking load of the hollow RC beams (W_{cr}) was calculated using the equation

$$\{W_{cr}\} = \frac{2}{a_v} x \frac{f_{cr} I_{cr}}{D - C} \quad (3.1)$$

Where

a_v = shear span

f_{cr}= modulus of rupture value of concrete

I_{cr}= Moment of inertia of cracked section

D = Overall depth

C = Depth of horizontal centroidal axis

Assumptions:

The following assumptions were made in the development of the theoretical model.

1. Sections that are plane before bending remain plane after bending.
2. At ultimate load, the stress distribution in concrete is rectangular in the compression zone.
3. The average compressive stress in concrete is taken as two-thirds of the cube compressive strength of concrete.
4. The maximum compressive strain in concrete is 0.0035.
5. The circular hole is treated as a square hole that has the same area wherever simplification in calculation is needed.
6. The tensile strength of concrete is neglected.
7. When the beam is carrying the ultimate load, tension steel has yielded.

III. RESULTS AND DISCUSSION

A. Results Presentation

The equations for predicting the first crack loads for RC rectangular hollow cored beams have been obtained for the present study and the previous research work and is summarized as equation 2.1 and equation 3.1 respectively.

i. First crack model equations for hollow cored rectangular beams

Table 4.2 is comparing the present study with the research work of the other researcher. The thirteen Beams have beam given a different Beam designation as shown in Table 4.1, $P_{cr,T}$, $P_{cr,PS}$, r%, and $\frac{P_{cr,T}}{P_{cr,PS}}$ are the theoretical values of the first crack load for the research work, the numerical First crack load values for the present study, percentage difference in the first crack load between the research work and this present study, and the ratio of the first crack load theoretical values to the present study values respectively.

ii. Discussions on the results of the theoretical study and the values of the present study for the first crack load

Table 4.1 represents the comparism of the first crack equations for the present study and the previous research carried out by Murugesan and Narayanan, 2016, designated as $P_{cr,PS}$ and $P_{cr,T}$ respectively. The effect of holes on the first crack loads for rectangular RC beam sections have been predicted conservatively using the proposed finite element method formulation by equating the numerical predicted first crack load with the

The average value of the ratio between the proposed numerical value and that proposed by Murugesan and Narayanan, 2016 was found to be 0.965 with a standard deviation of 0.025 and coefficient of variation of 2.576. Therefore, it is possible to predict the first crack load of hollow cored beams using numerical methods and incorporating the modulus of rupture of the concrete with a conservative value close to experimental results.

modulus of rupture of the concrete. Comparisms have been made of the proposed numerical first crack load and that developed by Murugesan and Narayanan, 2016.

For control beam CB1, and beams B1, B2, and B3, there was a decrease in first crack load from 23.3kN to 20.6kN, and from 23.1kN to 21.9kN for Murugesan and Narayanan, 2016 and the Present study respectively. There was also a decrease in first crack load for Beams B4, B5, and B6 from 21.6kN to 21.2kN and from 22.8kN to 22.4kN for Murugesan and Narayanan, 2016 and the Present study respectively, after the load increased from 20.6kN (B3) to 21.6kN(B4) and from 21.9kN(B3) to 22.8kN(B4) for Murugesan and Narayanan, 2016 and the Present study respectively. Beams B7, B8, and B9 showed a decrease in first crack load for Murugesan and Narayanan, 2016 and the Present study from 22.0kN to 21.7kN and from 22.8kN to 22.6kN respectively.

The values of the first crack load increased from 21.7kN(B9) to 22.6kN(B10) for Murugesan and Narayanan, 2016 and for the present study showed an increase from 22.6kN(B9) to 22.8kN(B10). Beams B10, B11, and B12 showed a decrease in first crack load of 22.6kN, 22.2kN, and 21.8kN for Murugesan and Narayanan, 2016 and 22.8kN, 22.3kN, and 21.8kN for the present study.

There appeared to be an increase in first crack load at points of transition from B3 to B4, B6 to B7, and B9 to B10 as a result of the drop in the hole diameter from 50mm to 25mm in all cases. It was observed that for both studies there was a decrease in first crack load as the hole diameter increased. Consequently, as the hole diameter dropped to 25mm from 50mm, the first crack load is expected to increase.

Plate 4.1, plate 4.2, and plate 4.3 are the pictures showing first crack on the hollow cored beams that emanated due to the point loads on the beam types.

Table 4.1. Beam specifications (Source: Orie and Ogbonna, 2024)

D_m (mm)	Type 1 beams		Type 2 beams		Type 3 beams	
	Width, b (mm)	Depth, h (mm)	Width, b (mm)	Depth, h (mm)	Width, b (mm)	Depth, h (mm)
0	150	150	150	150	150	150
30	150	150	150	155	155	150
60	150	150	150	165	165	150
75	150	150	150	175	175	150
105	150	150	150	201	201	150

Table 4.2. Details of Beams (Source: Murugesan and Narayanan, 2016)

Serial Number	Beam Designations	Diameter of hole (mm)	Distance of centre of hole from top Surface (mm)	Beam cross section (widthxheight, mm)	***Mode of Failure***	***Cube Strength of Concrete (N/mm²)***
1	CB1	0	0	150x250	Flexure	26.30
2	B1	25	45	150x250	Flexure	25.32
3	B2	40	45	150x250	Flexure	25.32
4	B3	50	45	150x250	Flexure	25.32
5	B4	25	65	150x250	Flexure	25.98
6	B5	40	65	150x250	Flexure	25.98
7	B6	50	65	150x250	Flexure	25.98
8	B7	25	55	150x250	Flexure	25.87
9	B8	40	55	150x250	Flexure	25.87
10	B9	50	55	150x250	Flexure	25.87
11	B10	25	180	150x250	Flexure	26.23
12	B11	40	180	150x250	Flexure	26.23
13	B12	50	180	150x250	Flexure	26.23

Table 4.3. Comparism of the results of the Present Study with the results of Murugesan and Narayanan, 2016 for the First crack model equations

Serial Number	Beam Designations	$P_{cr,T}$ kN	$P_{cr,PS}$ kN	$\frac{P_{cr,T}}{P_{cr,PS}}$	*r%*
1	CB1	23.3	23.1	1.009	0.858
2	B1	21.2	22.5	0.942	5.778
3	B2	20.9	22.2	0.941	5.856
4	B3	20.6	21.9	0.941	5.936
5	B4	21.6	22.8	0.947	5.556
6	B5	21.4	22.6	0.947	5.310
7	B6	21.2	22.4	0.946	5.357
8	B7	22.0	22.8	0.965	3.636
9	B8	21.9	22.7	0.965	3.524
10	B9	21.7	22.6	0.960	3.982
11	B10	22.6	22.8	0.991	0.877
12	B11	22.2	22.3	0.996	0.451
13	B12	21.8	21.8	1.000	0
			Mean	0.965	3.493
			Standard Deviation	0.025	
			Coefficient of variation	2.576	

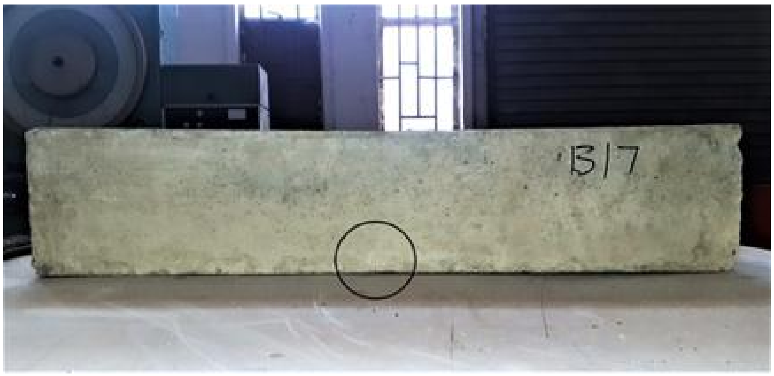

Plate 4.1: *Picture showing first crack on the hollow cored Beams that emanated due to the point load on a Type 1 Beam.(Source: Orie and Ogbonna, 2024).*

Plate 4.2: *Picture showing first crack on the hollow cored beams that emanated due to the point load on a Type 2 Beam. (Source: Orie and Ogbonna, 2024).*

Plate 4.3: *Picture showing first crack on the hollow cored beams that emanated due to the point load on a Type 3 Beam. (Source: Orie and Ogbonna, 2024).*

IV. CONCLUSIONS AND RECOMMENDATIONS

A. Conclusions

Analytical and Finite element equations have been derived by Murugesan and Narayanan, 2016, and this present study respectively for determining the first crack load of hollow-cored RC beams using their modulus of rupture. Based on the results from the comparism between the research work carried out by Murugesan and Narayanan, 2016 and that of the present study, the values of the first crack load equations are found to be in good agreement.

B. Recommendations

This research employed the application of finite element method in the prediction of the first crack load of Hollow-cored beams by applying a numerical equation developed by Orie and Ogbonna, 2024 and incorporating the modulus of rupture of the concrete. Researchers, Engineers and Professionals can adopt the model equations in their Engineering designs as the results agree with the previous work done.

REFERENCES

Agag, F.M.F., Ahmad,S.S.E., and Sallam, H.M. (2022). Experimental assessment of different strengthening techniques for opening in reinforced concrete beams. Frattura ed Integrità Strutturale, 59, pp. 549-565; DOI: 10.3221/IGF-ESIS.59.36.

Berrocal, C.G., Fernandez, I., and Rempling, R. 2020. Crack monitoring in reinforced concrete beams by distributed optical fiber sensors.Structure and Infrastructure Engineering Maintenance, Management, Life- Cycle Design and Performance. https://doi.org/10.1080/15732479.2020.1731558.

Bharikatti, S. S. "Finite Element analysis", 1st edition, New age international (P) ltd., New Delhi, India, 2005.
British Standards Institution, BS 1881 part 109. "Specifications for Concrete Moulds", *British Standards* BS 8110 part 2-Code of Practice for special circumstances.

Chin, S.N., Shafiq, N., and Nuruddin, M.F. (2015). FRP as strengthening material for reinforced concrete beams with openings - A review", KSCE Journal of Civil Engineering, vol. 19(1), pp. 213-219.

Concrete Mix Design Manual First Edition:Council for the Regulation of Engineering in Nigeria, special Publication; No. Coren/2017/0 16/RC, August 2017.

Fakoor, M., and Farid, H.M. (2018). Mixed-mode I/II fracture criterion for crack initiation assessment of composite materials, Acta Mech. https://doi.org/10.1007/s00707-018-2308-y
House, London, 1983.
Journal of the Civil Engineering Forum, 9(2):181-194.

Lia, D., Huanga, P., Chena, Z., Yaod, G., Guoa, X., Zhenga, X., and Yanga, Y. (2020). Experimental study on fracture and fatigue crack propagation processes in concrete based on DIC technology. Engineering Fracture Mechanics, 235, 1-19.

Ling, J.H., Leong, W.L., and Sia, H.T. (2020). Behaviour of Reinforced Concrete Beams with Circular transverse openings under static loads, Journal of Science And Applied Engineering (JSAE), Vol 3 (1), 1-16

Ling, J.H., Lim, Y.T., and Jusli, E. (2023). Methods to Determine Ductility of Structural Members: A Review, Journal of Civil Engineering Forum, 9(2), 181-194.

Ling, J.H., Tang, H.S., Leong, W.K., and Sia, H.T. (2019). "Effects of transverse circular opening in reinforced concrete beam subjected to incremental static load", Borneo Journal of Sciences and Technology, vol. 1(2),16-26.

Mohammed, S.I., and Najim, K.B. (2020). Mechanical strength, flexural behavior and fracture energy of Recycled Concrete Aggregate self-compacting concrete. Structures, 23, 34-43.

Mosley, W. H., and Bungey, J. H. Macmillan Education Ltd Reinforced Concrete Design, 1990.

NIS444-1. Composition, Specification, and Conformity Criteria for Common Cements, Standard Organization of Nigeria, Lagos, 2014.

Orie, O. U., and Ogbonna, U. K. (2024). Numerical Method for Predicting First Crack Load on Hollow-Cored Beams subjected to Point Load at Midspan. Nigerian Journal of Technology, 2024; 43(1), pp. 44 – 50; https://doi.org/10.4314/njt.v43i1.6.

Osman, B.H., Wu, E., Ji, B., and Abdelgader, A.M.S. (2016.)"A state of the art review on reinforced concrete beams with openings retrofitted with FRP", International Journal of Advanced Structural Engineering, vol. 8(3), 253-267.

Zhang, J., and Li, V.C. (2004). Simulation of crack propagation in fiber-reinforced concrete by fracture mechanics. Cement and Concrete Research 34:333 – 339